Neutrophil myeloperoxidase as a functional biomarker for RSV severity: implications for *in vitro* therapeutic screening.

Machaela Palor[1], Samuel Ellis[1], Amy I. Jacobs [1], Thomas Benoist[2], Paolo De Coppi[2], Jennifer L. Rohn[3], Gabriele Pollara[4], Robert E. Hynds[5], Rosalind L. Smyth[1], Samiran Ray[1,6], Claire M. Smith[1*]

Affiliations

1. Infection, Immunity and Inflammation, Great Ormond Street Institute of Child Health, University College London, London, U.K.
2. Stem Cell and Regenerative Medicine Section, Great Ormond Street Institute of Child Health, University College London, London, U.K.
3. Department of Renal Medicine, Division of Medicine, University College London, London, U.K.
4. Division of Infection and Immunity, University College London, London, U.K.
5. Epithelial Cell Biology in ENT Research (EpiCENTR) Group, Developmental Biology and Cancer Department, Great Ormond Street Institute of Child Health, University College London, London, U.K.
6. Paediatric Intensive Care Unit, Great Ormond Street Hospital for Children NHS Foundation Trust and NIHR Biomedical Research Centre, London, U.K.

* Corresponding author:

Dr Claire Mary Smith,

UCL Great Ormond Street Institute of Child Health,

30 Guilford St,

London WC1N 1EH

c.m.smith@ucl.ac.uk

Keywords: virus infection, endothelial cells, bronchial epithelial cells, paediatric infection

Abstract

Neutrophils play a dual role in respiratory syncytial virus (RSV) infection, contributing to both viral clearance and lung damage. Analysis of peripheral blood-derived neutrophils from infants with RSV admitted to the Paediatric Intensive Care Unit (PICU) at Great Ormond Street Hospital (GOSH) highlighted myeloperoxidase (MPO), a hallmark of neutrophil degranulation, as a key indicator of disease severity when compared to control infants. The aim of this study is to investigate MPO as a functional readout of therapeutic efficacy.

To mechanistically investigate these clinical observations, we developed a physiologically relevant *in vitro* model of the paediatric airway. Differentiated paediatric airway epithelial cells (AECs) were cultured at air-liquid interface (ALI), with or without an underlying layer of vascular endothelial cells. Following RSV infection, neutrophil migration and activation were assessed using flow cytometry. The inclusion of an endothelial layer enhanced physiological relevance and more accurately replicated *in vivo* MPO responses.

To evaluate the therapeutic modulation of neutrophil activation, two antiviral compounds—remdesivir (RDV) and RSV604—were evaluated. While both compounds significantly reduced RSV viral load at 24 hours post-infection, only RSV604 attenuated MPO expression. RDV had no measurable effect on MPO levels, suggesting limited efficacy in mitigating neutrophil-driven inflammation.

These findings highlight MPO as a biomarker of RSV severity and a functional readout of therapeutic impact. Targeting MPO-driven neutrophil activation may be key to reducing both viral load and inflammation.

Take home message: Antiviral drug discovery should include neutrophil MPO reduction as a readout of therapeutic efficacy.

Graphical Abstract

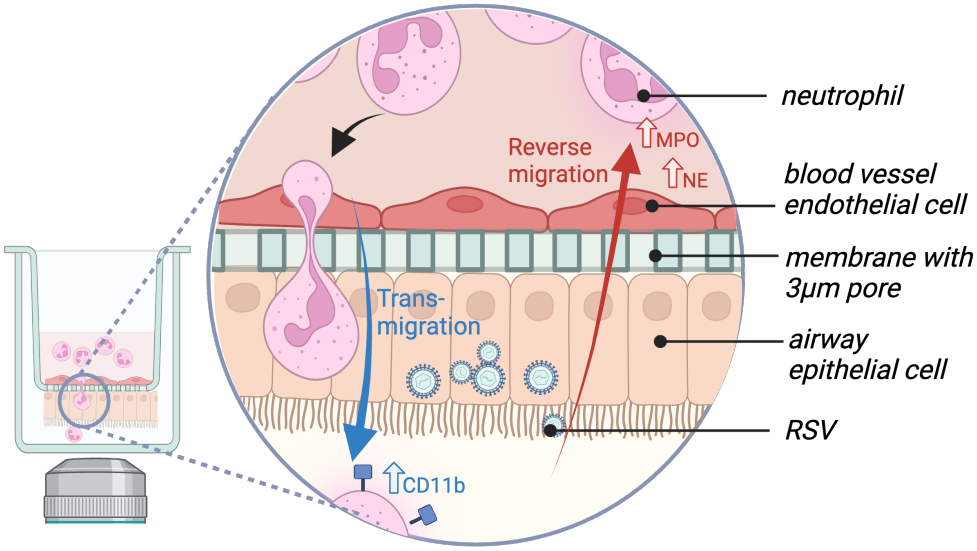

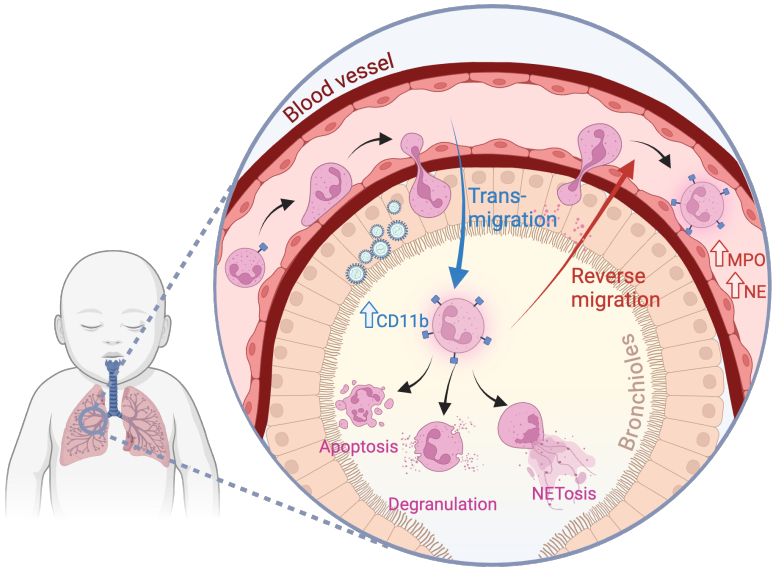

Introduction

Respiratory syncytial virus (RSV) is a leading cause of severe lower respiratory tract infections (LRTI) in infants and young children, resulting in approximately 3.2 million hospital admissions and an estimated 118,000 deaths in children under five years of age (1). Despite these substantial health impacts, current therapeutic options primarily focus on prevention and symptom management. Treatments available are limited to ribavirin, a rarely used antiviral due to its toxicity and cost (2); palivizumab, a monoclonal antibody requiring monthly dosing for high-risk infants (3, 4); and nirsevimab, a recently approved long-acting monoclonal antibody shown to provide extended protection with a single dose (5, 6). The lack of accessible, effective therapies highlights the need for continued advancements in RSV treatment and prevention.

Neutrophils are rapidly recruited to the lungs during RSV infection, playing a key role in the host defence mechanism by targeting the virus (7). However, excessive neutrophil infiltration and activation can contribute to airway inflammation, epithelial damage, and disease severity (8, 9). While mouse studies have shown that neutrophil activation primarily occurs within the lung environment during RSV infection (10, 11), others have shown that neutrophils in the systemic circulation of RSV-infected children also exhibit high levels of activation markers, indicating that their activation is not limited to the lung environment (12). Additionally, RSV proteins have been detected within these circulating neutrophils (12), raising the possibility that some neutrophils, after interacting with virus-infected cells in the lungs, may re-enter the bloodstream. This process of reverse migration could have significant implications for systemic inflammation and viral dissemination.

Understanding neutrophil behaviour during RSV infection, including during their migration across the airway epithelial barrier and activation, is crucial for developing therapeutic strategies to mitigate pathological inflammation without compromising the antiviral response. Studies have shown that trans-epithelial migration is essential for neutrophil activation during RSV infection, leading to increased expression of activation markers and release of inflammatory mediators (10, 11, 13). *In vivo* studies are limited by their complexity and ethical considerations, necessitating the use of *in vitro* models

that closely replicate the human airway environment, which can differ between children and adults (14). Differentiated airway epithelial cells (AECs) cultured at the air-liquid interface (ALI) provide a physiologically relevant platform to study neutrophil migration and the effect of antiviral treatments on this process. This approach is particularly valuable given the pressing need for robust pre-clinical models that can accelerate the development and optimisation of antiviral therapies.

In this study, we aimed to investigate neutrophil activation and degranulation in the context of RSV infection, using both clinical samples and a refined *in vitro* paediatric airway model. We analysed neutrophils from RSV-infected infants admitted to the Paediatric Intensive Care Unit (PICU) at Great Ormond Street Hospital (GOSH) and validated our clinical observations using a human trans-epithelial ALI migration model (10, 15). To enhance physiological relevance, we incorporated a vascular endothelial cell (EC) layer alongside differentiated AECs, enabling us to study early infection dynamics and neutrophil phenotype in a more representative airway environment. Finally, we evaluated the effects of two repurposed antiviral therapies—remdesivir (RDV), a broad-spectrum nucleoside analogue, and RSV604, a small-molecule RSV fusion inhibitor—on neutrophil migration, priming, and degranulation, to assess their potential in modifying immune responses during RSV infection.

Methods

Neutrophil Isolation and Purification

Ethical approval was obtained from the Living Airway Biobank (19/NW/0171; UCL_CS_23A) for paediatric patients admitted to the GOSH PICU with an indwelling arterial or a central venous line or UCL Research Ethics Committee (Project ID number: 19165/001) for the collection of venous blood from healthy adult volunteers. Written informed consent was obtained directly from donors, or their guardian and blood sampling was carried out by trained phlebotomists.

Neutrophils were isolated from RSV-infected (n = 5, age range 1.5–29 months, 60% female) and control (n = 5, age range 0.2–7 months, 80% female) paediatric patients (**Fig. 1a–c**; detailed patient characteristics in **Table 1**) or healthy adults (n = 15, aged 20-40 years, 58% female). Neutrophils were isolated using the EasySep™ Direct Human Neutrophil Isolation Kit (#19666, STEMCELL Technologies, UK), yielding approximately 1 x 10^7 neutrophils with up to 99% purity. Briefly, the sample was incubated with 500 µl of the Isolation Cocktail and RapidSpheres™, followed by a magnetic separation in 50 ml of cell separation buffer. The clear fraction was collected, re-incubated with RapidSpheres™, and placed on a magnetic stand. After further incubation and centrifugation at 300 x g, the pellet was resuspended in separation buffer and further enriched using the EasySep™ Human Neutrophil Isolation Kit (#17957, STEMCELL Technologies, UK) as per the manufacturer's instructions.

Airway Epithelial Cell (AEC) Culture and Differentiation

Primary paediatric (2-year-old female Caucasian) bronchial AECs were purchased from Epithelix Sàrl (Geneva, Switzerland) and co-cultured on mitotically inactivated 3T3-J2 feeder cells as described previously (16, 17). Cell stocks were frozen down at 1 x 10^6 cells/100 µl in Bambanker™ BB01 (NIPPON Genetics, Germany), a serum-free cryopreservation medium.

AECs were then cultured at ALI in complete PneumaCult™-ALI medium (STEMCELL Technologies, Vancouver, Canada) for 28 days to promote differentiation as described

previously (18). ALI cultures with trans-epithelial electrical resistance (TEER) of 200 $\Omega*cm^2$ or greater were used for experiments.

Endothelial Cell Culture

Human umbilical vein endothelial cells (HUVECs) transduced with ETS variant transcription factor 2 (ETV2), also known as 'reset' vascular ECs (19), were cultured on recombinant laminin-511 E8 fragment-coated flasks (iMatrix-511, AMSBIO, UK) in endothelial growth medium (EGM) composed of complete Endopan 300 SL medium (Pan BioTech, Germany) and 5% human serum (HS) (Merck, Darmstadt, Germany). Cell stocks were frozen down at 1 x 10^6 cells/ml in EGM supplemented with 40% HS and 10% DMSO.

For co-culture at ALI, ECs were seeded into membrane inserts at 3.5 x 10^4 in 100 µl complete PneumaCult™-ALI medium supplemented with iMatrix-511 (1.5 µg/cm^2) and incubated for 24 hours prior to performing dextran permeability assays or neutrophil migration experiments.

Dextran Permeability Assay

To assess cell barrier integrity, membrane inserts with ALI AEC cultures alone or in co-culture with ECs, were placed in Hanks' balanced salt solution containing calcium and magnesium (HBSS+/+) plus Texas Red™-dextran (Thermo Fisher Scientific, UK) at 100 µg/ml for 20 minutes in the dark. 100 µl of standards and supernatant were transferred to a solid black 96-well plate in triplicate and fluorescence was measured with a BMG FLUOstar OMEGA microplate reader at an excitation/emission wavelength of 595/615 nm. A membrane without cells served as a control. The translocated dextran concentration, derived from a standard curve, indicated paracellular permeability.

Viral Infection and Quantification

Recombinant GFP tagged-RSV A2 strain was provided by Fix et al (20). ALI cultures were infected at a MOI of 1 in 25 µl HBSS+/+ for one hour at 37°C. The virus quantity was based

on an estimated 1 x 10^5 cells per membrane. Mock-infected controls received 25 µl HBSS+/+. After inoculation, the virus solution was removed, and cultures were incubated for 24 hours with replenished basolateral ALI medium.

For quantification, viral RNA was extracted from apical supernatants using the QIAamp Viral RNA Mini Kit (Qiagen, Germany). cDNA was synthesized from 100 ng RNA using the High-Capacity RNA-to-cDNA Kit (Thermo Fisher Scientific, UK) in a 40 µl reaction. RT-qPCR was performed using TaqMan Universal Master Mix II (Thermo Fisher Scientific, UK) with specific primers and a fluorescent probe for the RSV-A N protein as described previously (18). Samples were run on an AB Biosystems StepOnePlus Real-Time PCR System (Thermo Fisher Scientific, UK). Viral load was extrapolated from a standard curve generated by performing ten-fold serial dilutions of a plasmid containing the N protein sequence starting at 1 x 10^6 copies to 1 copy (21).

Trans-epithelial Migration Assay

On the day of the neutrophil migration assay, ALI cultures were incubated with 600 µl HBSS+/+ for one hour at 37°C to collect immunomodulatory factors. Supernatants were collected, centrifuged, and 400 µl was transferred to a 24-well plate with ALI cultures. Purified neutrophils were diluted to 5 x 10^6 cells/ml in HBSS+/+ with 1% (v/v) autologous human serum. 100 µl was added basolaterally to each membrane insert and incubated for one hour at 37°C.

Assessment of Neutrophil Markers and Degranulation

After migration, neutrophils (apical, adherent, basolateral) were collected, centrifuged, blocked with Human TruStain FcX™, and stained with LIVE/DEAD™ fixable violet dye (Thermo Fisher Scientific, UK). Following washing, cells were stained with 1/50 dilution of CD11b-FITC (Miltenyi Biotec, 130-110-552), CD64-APC-Cy7 (Miltenyi Biotec, 130-116-199), and CD62L-PE-Cy7 (Miltenyi Biotec, 130-129-810) for 20 minutes at 4°C in the dark. Cells were washed, fixed with PFA, permeabilised, and stained intracellularly with MPO-APC (Miltenyi Biotec, 130-119-786) and NE-PE (Santa Cruz Biotechnology, sc-55549 PE).

After a final wash, neutrophils were resuspended in FACS buffer and analysed using a CytoFLEX S flow cytometer, obtaining mean fluorescence intensity (MFI) values for CD11b, CD64, CD62L, MPO, and NE from the CD11b-positive gated population. Data are presented as raw MFI values, or as log fold change from controls. To visualize patterns of marker expression, we utilized a Quartile Score, where the mean MFI of each marker was categorized into quartiles (0–3); 0 corresponds to the lowest quartile and 3 to the highest, calculated across all compartments and experimental conditions. Associations between marker expression patterns across different compartments or conditions of the model were visualised using `radarcharts` generated with the `fmsb` R package (22). Here, the centre of each plot represents the lowest level of marker expression, while points closer to the edges indicate higher expression levels. The individual quartile scores were totalled to calculate a Combined Quartile Score for each condition. Statistical analyses were performed using Wilcoxon signed-rank tests, with adjustments for multiple comparisons to control the false discovery rate.

Neutrophil elastase activity in supernatants was measured using the Neutrophil Elastase Activity Assay Kit (Cayman Chemical, USA) as per the manufacturer's instructions. Samples were diluted 1/10, incubated with elastase substrate, and fluorescence was measured at 485/525 nm with a BMG FLUOstar OMEGA microplate reader.

For MPO activity, samples were diluted 1/2 and incubated with 3,3',5,5'-Tetramethylbenzidine (TMB) substrate as described using the Neutrophil MPO Activity Assay Kit (Cayman Chemical). Absorbance was measured at 650 nm with a BMG FLUOstar OMEGA microplate reader.

Cytokine Measurement

The BD Cytometric Bead Array (CBA) assay (BD Biosciences, USA) was used to quantify human soluble proteins, including key mediators of inflammation and neutrophil migration, IL-6, CXCL8 (IL-8), and CXCL10 (IP-10) (23, 24), in supernatants from mock- or RSV-infected cultures. Following the manufacturer's protocol, a standard curve was generated, and test samples were diluted 1/10 in assay diluent. Standards and samples were incubated with capture beads for one hour, followed by PE detection reagent for two

hours. After washing, the beads were resuspended in wash buffer and analysed using a BD FACSymphony A5 flow cytometer (BD Biosciences, Franklin Lakes, NJ, USA).

Antiviral Treatment

RSV-infected bronchial AECs were treated with a broad-spectrum antiviral remdesivir (RDV, Bio-Techne, USA) or RSV-specific antiviral compound, RSV604 (Cambridge Bioscience, UK), which has high efficacy in inhibiting RSV replication (25). RDV (Bio-Techne, USA) and RSV604 (Cambridge Bioscience, UK) were diluted in ALI medium to working concentrations of 6.6 μM and 10 μM, respectively, and added to the basolateral side at four hours post-infection. AECs were used for neutrophil migration experiments at 1 day post infection (dpi). The effects of the antiviral on RSV-induced neutrophil migration and receptor expression were assessed by comparing treated and untreated cultures. Additional infected AECs with and without antiviral treatment were recorded for viral GFP fluorescence using a Nikon Ti-E microscope up to 7 dpi.

Statistical Analyses

Data were analysed and visualized using GraphPad Prism v10.0 or RStudio 2023.09.1+494. It is important to note that there was considerable variability (>1 log) in baseline neutrophil marker expression across different donors (**Supplementary Fig. 2a**). This variability likely reflects inherent differences in neutrophil states between individuals at collection. To account for this in our analysis, we present our data as the mean fold change in MFI relative to neutrophils cultured only in medium ('medium-only') for each condition. This approach normalized the individual baseline differences and allowed us to focus on the migration-dependent effects.

Normality was assessed with the Shapiro-Wilk test. For normally distributed data, a student's t-test (two groups) or One-way ANOVA with Bonferroni correction (three or more groups) was used. Two-way ANOVA with Tukey correction was applied for comparisons involving two factors. Non-normally distributed data were analysed with Mann-Whitney U or Wilcoxon signed-rank tests (two groups) and Kruskal-Wallis or Friedman tests with Dunn's post-hoc for unpaired or paired data, respectively. Results

are presented as mean ± SEM unless specified otherwise. Statistical significance was set at $P < 0.05$.

Results

Enhanced Neutrophil Degranulation in the Blood of RSV-Infected Infants

We examined peripheral blood neutrophils from infants admitted with RSV at GOSH ICU for similar neutrophil marker expression patterns. Neutrophils were isolated from RSV-infected (n = 5, age range 1.5–29 months, 60% female) and control (n = 5, age range 0.2–7 months, 80% female) paediatric patients (**Fig. 1a–c**; detailed patient characteristics in **Table 1**). Baseline assessment of neutrophil morphology showed no significant differences in size (forward scatter, FSC) or granularity (side scatter, SSC) between groups (**Fig. 1d**). However, peripheral blood neutrophil counts were significantly lower in RSV-infected infants, with a mean viable cell count of 9.9×10^5 cells/mL compared to 2.6×10^6 cells/mL in control infants ($p < 0.05$) (**Fig. 1e**).

Flow cytometric analysis showed significantly increased MPO and NE expression in neutrophils from RSV-infected infants compared to controls ($p < 0.05$), whereas CD11b, CD62L, and CD64 levels did not differ significantly between groups **(Fig. 1f, g**). Correlation analysis revealed no significant associations between neutrophil markers in either group (**Fig. 1h**).

Radar plot analysis confirmed that MPO and NE were elevated in RSV patient neutrophils compared to controls, with other markers remaining unchanged (**Fig. 1i**). An odds ratio analysis showed that MPO and NE expression were the most strongly associated with RSV infection, with 95% confidence intervals indicating a significant likelihood of increased expression relative to controls (**Fig. 1j**).

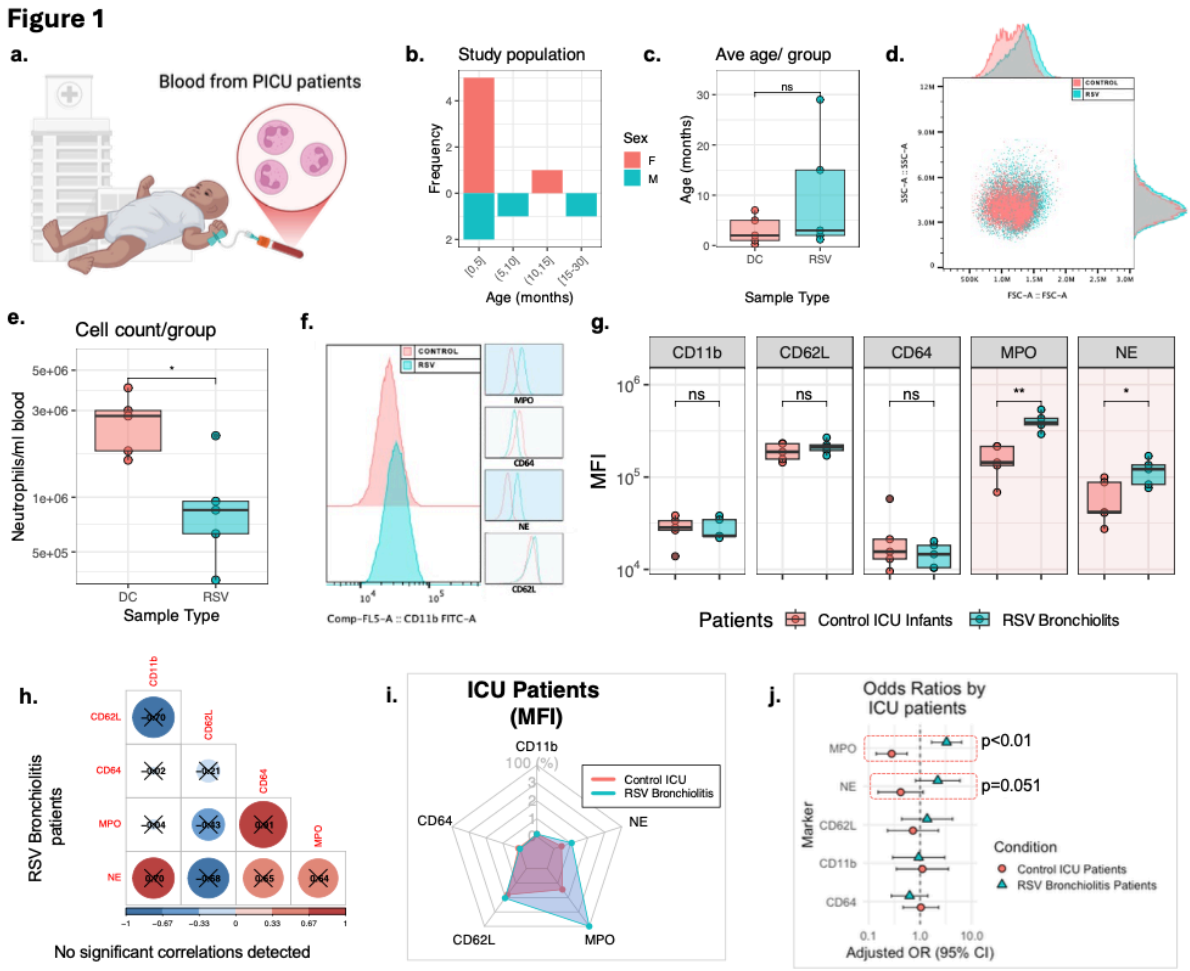

Figure 1 Neutrophil Marker Expression in Infants with RSV Bronchiolitis and uninfected Control ICU Patients. *(a) Schematic of study design showing blood sampling from infants with RSV bronchiolitis (RSV) and uninfected control ICU patients (DC). (b) Study population demographics by age group and sex (F = female, M = male). (c) Average age comparison between control (DC) and RSV patient groups. (d) Representative density plots showing neutrophil distribution in blood from control and RSV patients. (e) Blood neutrophil counts per group. RSV patients exhibit significantly lower neutrophil counts compared to controls (*p < 0.05). (f) Representative histograms showing neutrophil marker expression (MPO, CD64, NE, CD11b) in control vs. RSV patients. (g) Mean fluorescence intensity (MFI) of neutrophil markers. MPO (p < 0.01) and NE (p < 0.05) are significantly elevated in RSV patients; CD11b, CD62L, and CD64 show no significant differences. (h) Correlation matrix of neutrophil marker expression in control and RSV patient groups; positive (red) and negative (blue) correlations are shown, X = non-significant. (i) Radar plots summarizing MFI of neutrophil activation markers (CD11b, CD62L, CD64, MPO, NE) in ICU patients; RSV patients show increased MPO and NE compared to controls. (j) Odds ratio plot showing relative likelihood of marker expression changes in RSV versus control patients; points represent odds ratios with 95% confidence intervals. Error bars represent standard deviation; ns = not significant; *p < 0.05, **p < 0.01.*

Endothelial Cells Modulate Cytokine Response and Neutrophil Migration Without Affecting RSV Replication

To further investigate the mechanisms underlying these patient responses, we utilised our *in vitro* model of neutrophil trans-endothelial epithelial migration during RSV bronchiolitis (18). Initial experiments showed that the addition of ECs to AEC cultures (timeline shown in **Fig. 2a**) maintained a TEER reading above 200Ω*cm2 (**Supplementary Fig. 1a**) and significantly decreased dextran permeability across the membrane insert (**Supplementary Fig. 1b**). This suggests that ECs enhance the tightness and selective permeability of the epithelial barrier. Viral load measurements indicated no significant difference between the AEC models grown with or without ECs, suggesting that ECs do not affect RSV replication (**Fig. 2b**). However, the cytokine response—including key mediators of inflammation and neutrophil migration, IL-6, IL-8, and IP-10—was significantly lower in the presence of ECs compared to conditions without ECs (**Fig. 2c,d** and **Supplementary Fig. 2**). Post-migration, viral load remained comparable between models with and without ECs; however, IL-6, IL-8, and IP-10 concentrations were significantly higher in the apical compartment when ECs were present (**Fig. 2e/f** and **Supplementary Fig. 3**). This suggests that ECs contribute to the development of a more pro-inflammatory environment through their interaction with neutrophils.

Although the addition of ECs had no effect on the overall number of viable neutrophils recovered from the membrane insert (**Fig. 2g/h**), ECs significantly altered the distribution of neutrophils following migration. In conditions without ECs, more neutrophils were found in the basolateral compartment following RSV infection, whereas in the presence of ECs, this distribution shifted, with a greater number of neutrophils detaching from the AECs and migrating to the apical compartment (**Fig. 2i**). This suggests that migration through ECs reduces adherence of neutrophils to AECs, potentially accelerating their movement toward the apical side, without impacting the total number of viable neutrophils recovered.

Endothelial Cells Enhance Neutrophil Degranulation Marker Expression and the Cytokine Response Following Trans-Epithelial Migration During RSV Infection

Analysis of neutrophil markers revealed that expression patterns were largely shaped by their compartmental location during migration, rather than by infection or the presence of ECs (**Fig. 2j**). Using paired analysis between mock and RSV infection conditions, we showed that neutrophil priming (CD11b) and degranulation markers (MPO and NE) were differentially expressed depending on the presence or absence of ECs. In the absence of ECs, RSV infection significantly increased CD11b expression in neutrophils in the basolateral compartment, while MPO and NE expression were significantly reduced compared to mock conditions. CD62L and CD64 expression remained unchanged (**Fig. 2j**). In the adhered AEC compartment, RSV infection led to a significant increase in CD11b expression, but no other markers showed significant changes (**Fig. 2j**). Neutrophils that migrated to the apical side displayed no significant differences in marker expression between RSV-infected and mock conditions (**Fig. 2j**).

In the presence of ECs, RSV infection led to significant upregulation of MPO and NE expression on neutrophils recovered from the basolateral compartment, while CD11b, CD62L, and CD64 remained unchanged from the mock (**Fig. 2j**). Notably, in the fully migrated neutrophils, RSV infection significantly increased CD11b expression, with no significant changes observed in the other markers. These results indicate that ECs selectively influence certain neutrophil degranulation markers, particularly MPO and NE, during RSV infection while having minimal impact on other markers.

We then analysed the patterns of neutrophil marker expression across different compartments to assess how RSV infection and the presence of ECs influenced their expression and coordination. The radar plots (**Fig. 2k**) illustrate these expression patterns across different compartments of the model. The centre of each plot represents the lowest level of marker expression, while points closer to the edges indicate higher expression levels. Across both models (No EC and EC), RSV infection (blue) consistently induces the highest quartile scores for neutrophil marker expression compared to baseline (green) or mock conditions (red), underscoring RSV infection as the principal driver of these changes. CD64 and CD62L expression is most pronounced in basolateral compartments, while CD11b, MPO, and NE are more elevated in adhered AEC and migrated compartments.

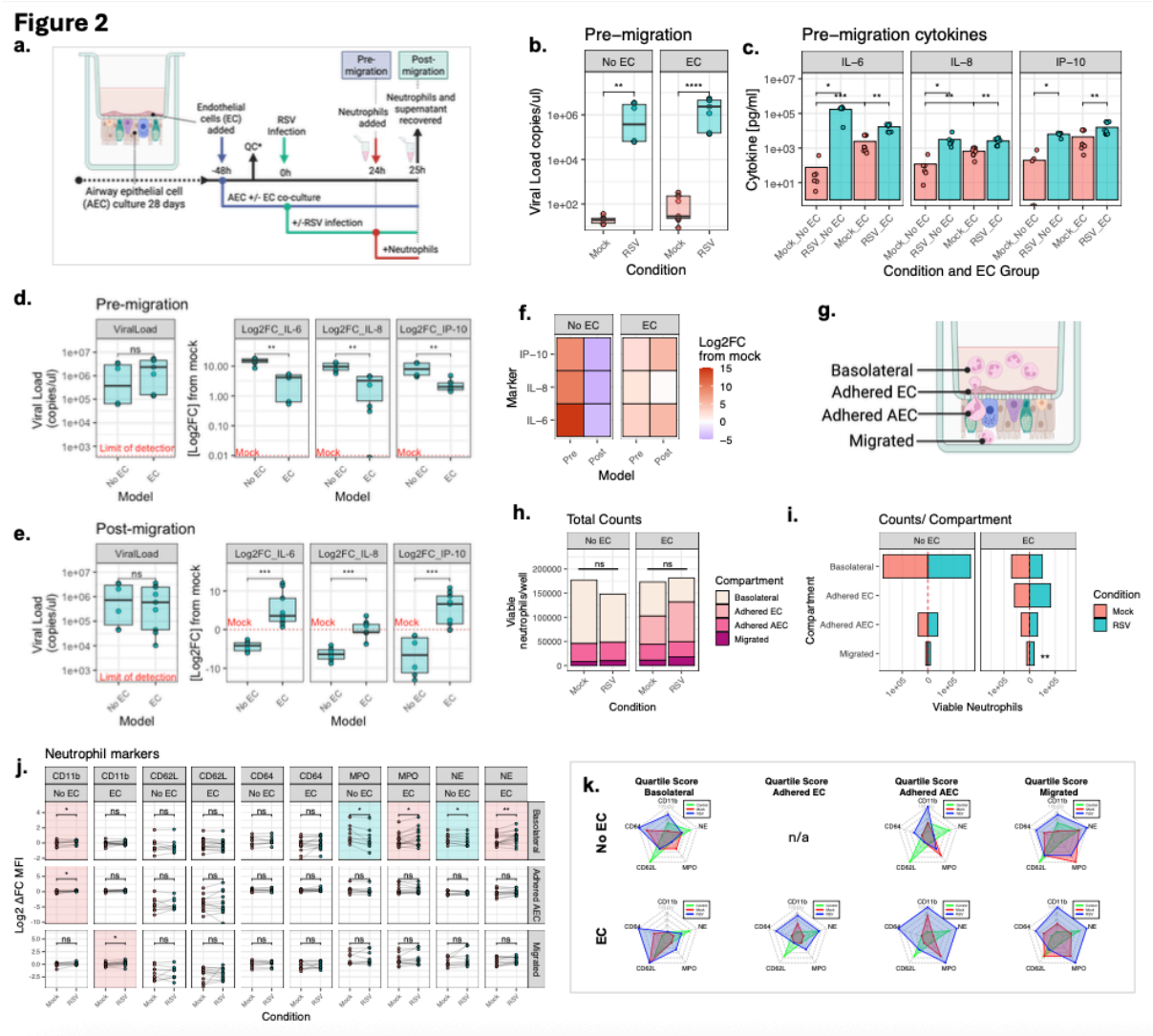

Figure 2 Impact of Endothelial Cells (EC) on RSV Infection, Barrier Integrity, and Neutrophil Response. *(a) Schematic and timeline of airway epithelial models with apical RSV infection for 24 h. (b) Viral load (copies/µl) post-neutrophil migration shows no significant difference (ns) between No EC and EC models. (c) Cytokine levels (log2 fold change from mock) for IL-6, IL-8, and IP-10 post-migration are significantly higher ($p < 0.001$) in EC models compared to No EC. (d) Viral load (copies/µl) post-RSV infection shows no significant difference between No EC and EC models. (e) Cytokine levels (log2 fold change from mock) for IL-6, IL-8, and IP-10 are significantly lower ($p < 0.01$) in the EC model compared to No EC post-RSV infection. (f) Schematic showing neutrophil migration across compartments in the airway epithelial model with EC. (g) Neutrophil distribution across compartments: in the No EC model, more neutrophils adhere to airway epithelial cells (AECs), while in the EC model, increased neutrophil presence is observed in the apical compartment with RSV infection ($p < 0.05$). (h) Neutrophil marker expression (log2 ΔΔFC of MFI) across compartments (basolateral, adhered to AECs, adhered to ECs, migrated neutrophils). Significant increases in MPO and NE expression are observed in the EC model ($p < 0.05$). (i) Radar plots showing quartile scores of neutrophil activation markers (CD11b, CD62L, CD64, MPO, NE) across compartments and in medium-only controls (green), mock-infected (red), and RSV-infected (blue) conditions. Error bars represent standard deviation; ns = not significant; *$p < 0.05$, **$p < 0.01$, ***$p < 0.001$.*

Basolateral MPO and NE Increases in Response to RSV Infection: Biomarkers of Reverse Migration

An odds ratio analysis revealed that most neutrophil marker expression was primarily influenced by the compartment from which neutrophils were recovered; however, distinct separation in odds ratios for MPO and NE in the basolateral compartment indicated that their expression was more directly influenced by RSV infection itself (**Fig. 3a**). To investigate whether these effects were driven by soluble factors from ECs or RSV-infected airway epithelial cells (AECs)—independent of neutrophil trans-epithelial migration—AECs were cultured on membranes with either permissive (3.0 μm pores) or blocked (0.4 μm pores) inserts (**Fig. 3b**). The smaller pores prevent neutrophil migration while still permitting passive diffusion of soluble factors.

Correlation analysis demonstrated significant positive associations between MPO and NE, and between NE and CD64, in migrated neutrophils under RSV infection (**Fig. 3c**), suggesting co-expression of these markers during reverse migration. No significant correlations were detected under blocked conditions (**Fig. 3d**) or in mock-infected controls (**Supplementary Fig. 4**). Radar plot analysis further showed that neutrophils in the blocked (0.4 μm) model exhibited lower activation scores across all markers compared to permissive cultures, irrespective of infection status (**Fig. 2e**).

Using this system, basolateral neutrophils exhibited significantly higher MPO and NE expression in RSV-infected cultures compared to mock controls under permissive (3.0 μm) conditions ($P < 0.05$), whereas no difference was observed under blocked (0.4 μm) conditions (**Fig. 3f**). Neutrophils recovered from RSV-infected cultures with blocked inserts exhibited CD11b, CD62L, MPO, and NE levels that were at least threefold lower than those recovered from permissive cultures (Fig. 2d). Interestingly, CD62L levels were higher in neutrophils exposed to RSV-infected AECs under blocked conditions, despite the absence of transmigration (**Fig. 3f**).

These findings suggest that MPO and NE upregulation in basolateral neutrophils is dependent on direct contact with RSV-infected AECs—consistent with reverse

migration—rather than solely due to soluble infection-related factors. The odds ratio analysis (**Fig. 3g**) supports this interpretation, revealing that MPO and NE expression is dependent on neutrophil migration and shows a marked separation of odds ratios between pore sizes.

Finally, ELISA analysis confirmed that increased MPO expression corresponded with significantly elevated MPO enzymatic activity in basolateral supernatants following neutrophil migration across RSV-infected AECs ($P < 0.05$), while NE activity remained unchanged (**Fig. 3h**).

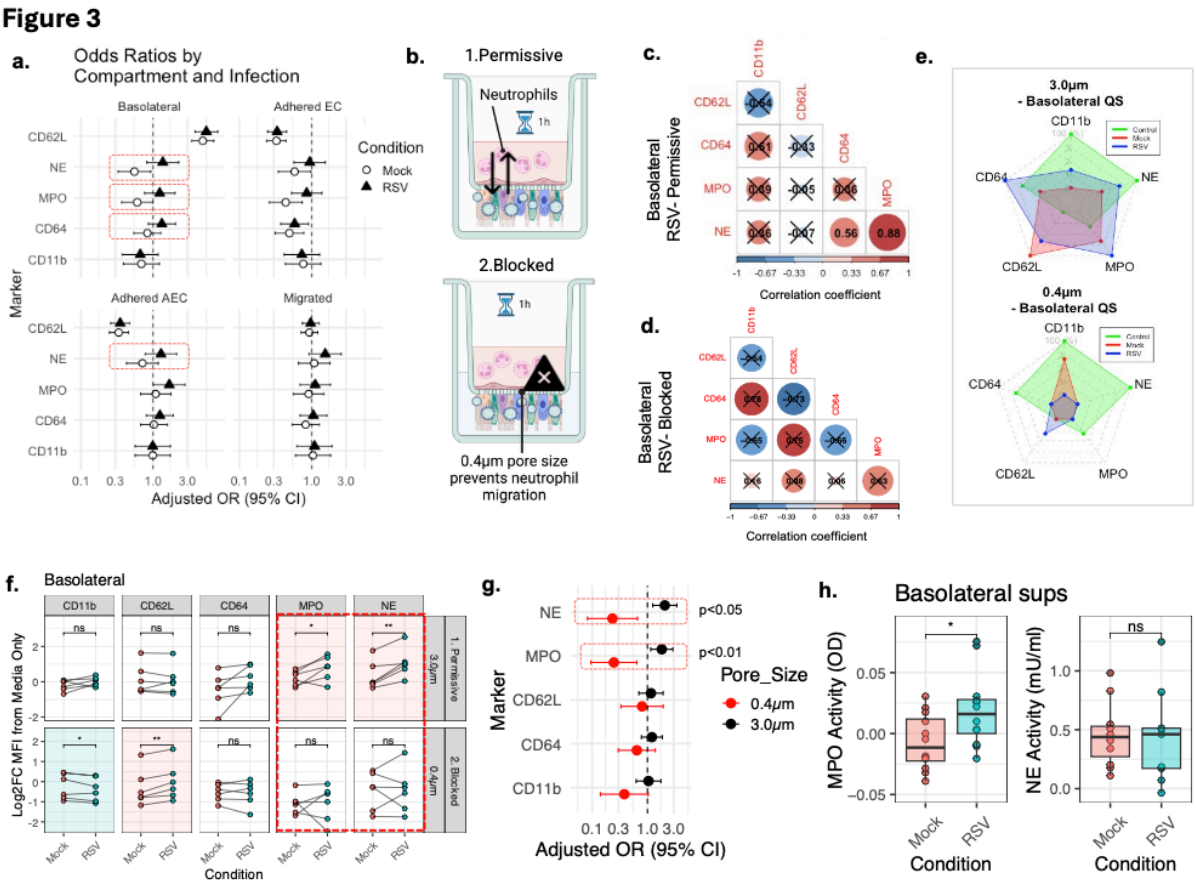

Figure 3 Neutrophil marker expression in response to RSV Infection in the basolateral compartment when neutrophils are permitted to migrate, or migration is blocked. *(a) Odds ratio plot showing the likelihood of neutrophils expressing specific activation and degranulation markers after transmigration across RSV-infected versus mock-infected epithelial monolayers. Points indicate odds ratios with 95% confidence intervals; black dots = RSV, white dots = mock. Red boxes indicate p<0.05. (b) Schematic of neutrophil migration assay using permissive (3.0µm pore size) and blocked (0.4µm pore size) models following 24 h RSV infection. (c, d) Correlation matrices of marker expression under permissive RSV (c) and blocked RSV (d) conditions. Positive (red) and negative (blue) correlations are displayed; strength is*

*indicated by circle size and colour intensity. X = non-significant correlations. (e) Radar plots showing quartile scores (QS) of neutrophil activation markers (CD11b, CD62L, CD64, MPO, NE) under permissive (3.0μm) and blocked (0.4μm) conditions. Blocking migration reduces scores for CD64 and MPO observed in RSV and mock infections under permissive conditions (*p < 0.05 compared to mock). (f) Log2 fold change (log2FC) from media-only control of MFI for individual markers (CD11b, CD62L, CD64, MPO, NE) under permissive and blocked conditions. RSV significantly increases MPO and NE expression under permissive conditions only (*p < 0.05, **p < 0.01). (g) Additional odds ratio plot showing the relative likelihood of marker expression changes under RSV vs. mock conditions in the basolateral compartment with 0.4μm or 3.0μm pore sizes. Points indicate odds ratios with 95% confidence intervals. Red boxes indicate p<0.05. (h) MPO and NE enzymatic activity in basolateral supernatants. RSV significantly increases MPO activity under permissive conditions (*p < 0.05), but no significant change is observed for NE activity (ns = not significant).*

Antiviral Treatments Reduce Viral Load but Enhance Baseline Inflammatory Cytokine Production

Next, we investigated the effects of two existing antiviral agents, remdesivir (RDV) and RSV604(25), on neutrophil-mediated inflammation (timeline shown in **Fig. 4a**), focusing on the production of IL-6, IL-8, and IP-10, as well as neutrophil marker expression. The structures of RSV604 (**Fig. 4b**) and RDV (**Fig. 4c)** are shown.

AECs were infected with GFP-tagged RSV and then incubated in the presence and absence of 10μM RSV604. In untreated controls, viral propagation was evident with increasing numbers of GFP-positive cells over a 7-day period, reflecting active infection and spread. In contrast, ALI cultures treated with RSV604 showed no detectable RSV-GFP infection throughout the entire time course, indicating that RSV604 effectively inhibits RSV replication and spread in this model (**Fig. 4d**). Similarly, ALI cultures treated with 6.6μM RDV also showed complete absence of GFP expression compared to untreated controls at 7 days post-infection, suggesting effective inhibition of RSV replication (**Fig. 4e**).

Apical supernatants collected following 24h RSV infection revealed a significant reduction in viral load following RDV ($1.2 \times 10^6 \pm 5.3 \times 10^5$ copies/μl) and RSV604 ($1.4 \times 10^6 \pm 5.0 \times 10^5$ copies/μl) treatment compared to untreated controls ($3.8 \times 10^6 \pm 6.7 \times 10^5$ copies/μl, $p<0.05$, $n = 6$) (**Fig. 4f**). These measurements, taken 24 hours post-infection, should be interpreted with caution since plaque assays at this time point were below the detection limit (data not shown), suggesting that the results may not reflect infectious viral load. Meanwhile, RSV infection resulted in a significant >5-fold increase in IL-6, and

IP-10 secretion relative to untreated controls (**Fig. 4e** and **Supplementary Figure 5**). RDV treatment with RSV infection significantly reduced IP-10 levels but had no effect on IL-8 or IL6. In contrast, RSV604 did not alter IL-6 or IP10 secretion but did lead to a decrease in IL8 levels with RSV infection.

Figure 4

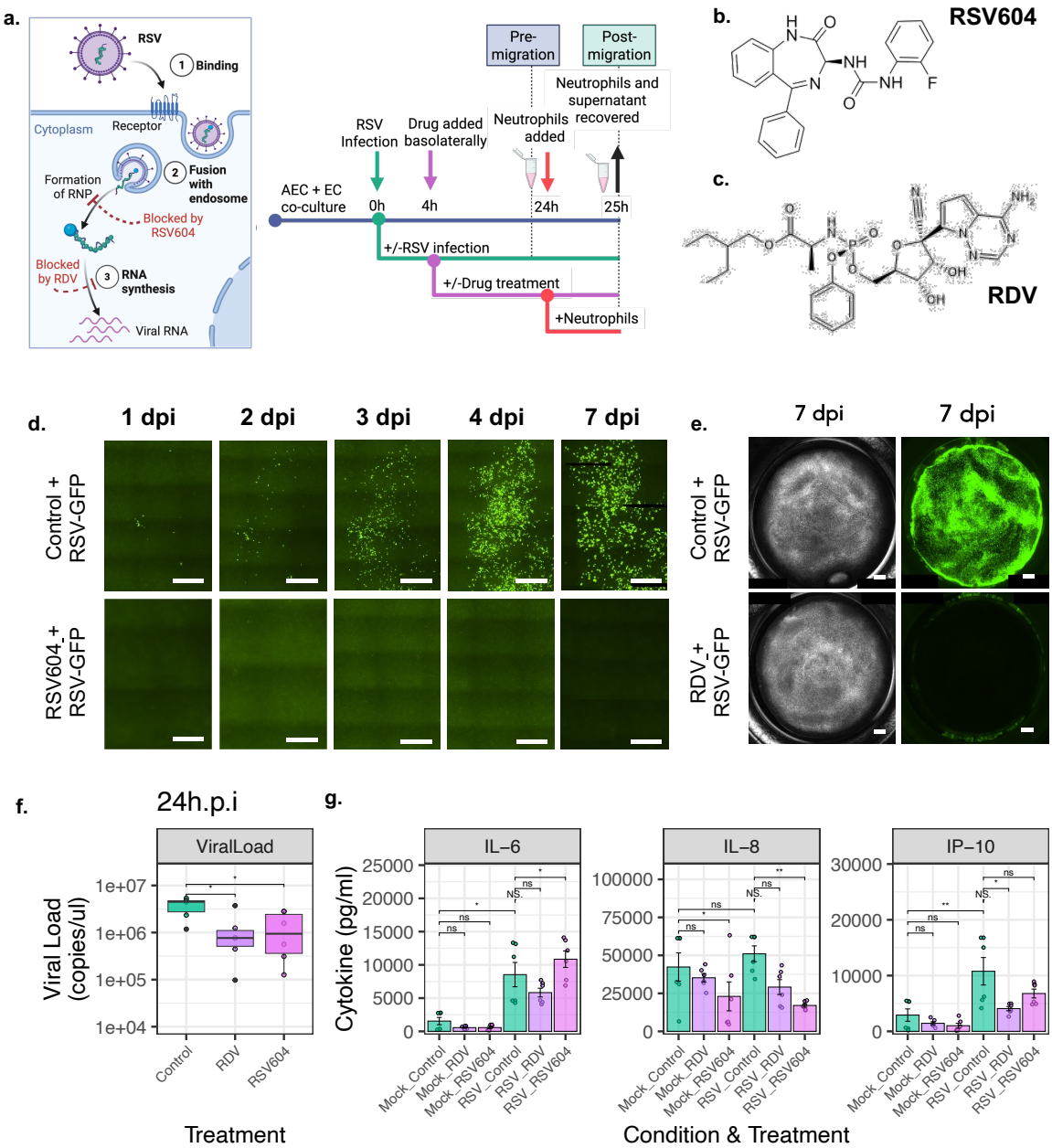

Figure 4 Effects of Antiviral Treatments on viral load and inflammation using in vitro RSV Models. *(a) Schematic of experimental design showing epithelial infection with RSV, antiviral treatments (RSV604, RDV), and neutrophil migration. Created with BioRender.com. (b, c) Chemical structures of RSV604 and RDV. (d) Representative micrographs showing inhibition of RSV-GFP infection of AECs up to 7 days post-infection (dpi) by 10μM RSV604. Scale bar = 300um (e) Representative brightfield (grayscale) and GFP (green) well-*

*scan micrographs show 6.6μM RDV inhibits RSV-GFP infection of AECs at 7 dpi. Scale bar = 10mm. (f) Pre-migration viral load in apical supernatants (copies/μl). RSV604 and remdesivir (RDV) significantly reduce viral load compared to RSV alone ($p < 0.05$). (g) Pre-migration apical cytokine levels (log2 fold change from mock) for IL-6, IL-8, and IP-10. RSV infection significantly increases cytokines; RSV604 and RDV further enhance these levels ($p < 0.05$). Error bars represent standard deviation; ns = not significant; *$p < 0.05$, **$p < 0.01$*

The Antiviral RSV604 Reduces Neutrophil-Mediated Inflammation During RSV Infection

We aimed to assess whether treatment with RDV (6.6μM) or RSV604 (10μM) could reduce the expression of key neutrophil degranulation markers, MPO and NE, which we found to be significantly elevated in both RSV infants and our *in vitro* model of RSV infection.

We found that RSV604 treatment was associated with a reduction in nearly all degranulation markers (**Fig. 5a,b**). While paired analyses comparing untreated and RSV604-treated basolateral neutrophils showed no significant differences (**Fig. 5c**), the radar plots (**Fig. 5b**) demonstrate that RSV604 (pink) markedly shifts neutrophil marker expression, particularly NE and MPO, across all compartments, aligning more closely with mock (red) conditions. This suggests RSV604's potential to effectively modulate the neutrophil response to RSV infection. In contrast, RDV (purple) shows weaker modulation, with marker expression patterns more closely resembling those of the RSV control (blue) or greater.

Notably, RSV604, but not RDV, increased the number of viable neutrophils on the apical side, either adhered to AECs or detached from the epithelium (**Fig. 5d**), suggesting that RSV604 may better preserve neutrophil viability post-migration and/or prevent reverse migration of neutrophils (**Fig. 5e**).

Odds ratio analysis identified MPO expression as the most significantly modulated marker in response to antiviral treatment (**Fig. 5c**). This was further supported by MPO enzymatic activity assays, which showed that RSV infection significantly increased MPO activity compared to mock controls ($p < 0.05$). While both RDV and RSV604 treatments reduced MPO activity relative to RSV alone, levels remained elevated compared to

mock, indicating partial but incomplete suppression of neutrophil degranulation (**Fig. 5f**).

This reduction in MPO activity was accompanied by changes in cytokine secretion following neutrophil migration. RDV treatment led to a significant decrease in IL-6 levels, whereas IL-8 and IP-10 remained unchanged. In contrast, RSV604 had no effect on IL-6 or IL-8 but induced a significant increase in IP-10 secretion (**Fig. 5g**). These findings suggest that while antiviral treatments can attenuate aspects of neutrophil activation, they do not fully restore inflammatory markers to baseline, highlighting the complexity of modulating immune responses during RSV infection.

Figure 5

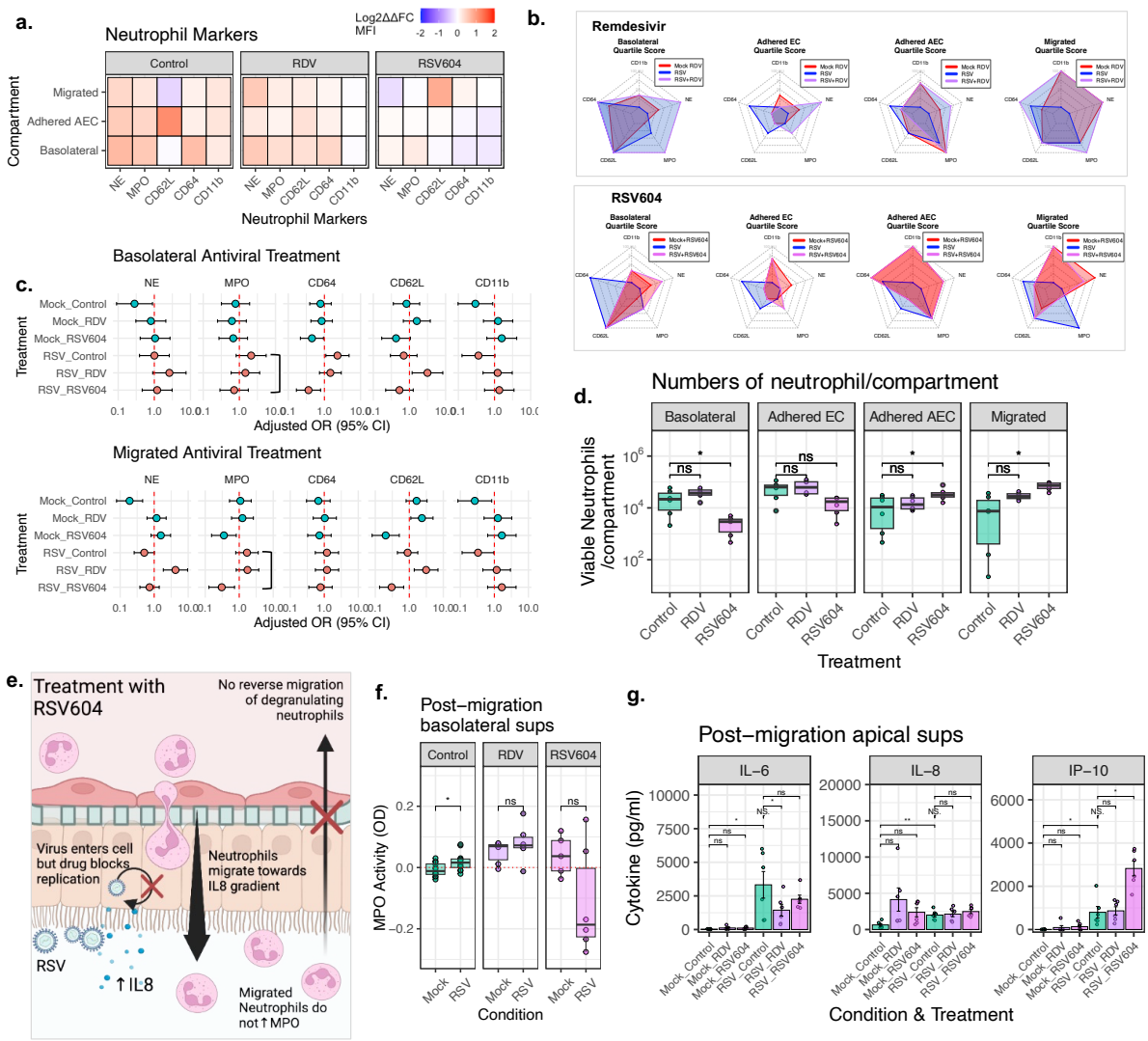

Figure 5 Effects of Antiviral Treatments on Neutrophil Degranulation using in vitro RSV Models. *(a) Heatmap showing neutrophil marker expression (log2ΔΔFC of MFI relative to medium-only and mock controls) across compartments and treatments. (b) Radar plots of neutrophil activation marker quartile*

*scores across compartments (basolateral, adhered epithelial, adhered endothelial, migrated neutrophils). RSV604 reduces MPO and NE activation, especially in migrated neutrophils. (c) Odds ratio plot showing likelihood of neutrophil marker expression under RSV versus control, and effects of antiviral treatments. Significant changes in the MPO OR indicated. (d) Total viable neutrophil counts across compartments. No significant differences (ns) in total neutrophil counts across treatments; RSV604 leads to increased migrated neutrophils. (e) Hypothesis depicting the effects of antiviral treatment on viral replication, cytokine secretion, and neutrophil transmigration. Created with BioRender.com. (f) MPO enzymatic activity in basolateral supernatants. RSV alone increases MPO activity ($p < 0.05$ vs. mock), while RSV604 and RDV prevent this increase. (g) Post-migration apical cytokine levels. RSV604 and RDV reduce IL-6, IL-8, and IP-10 compared to RSV alone ($p < 0.05$) and below mock levels. Error bars represent standard deviation; ns = not significant; *$p < 0.05$, **$p < 0.01$.*

Discussion

Clinically, elevated MPO and NE levels have been observed in bronchoalveolar lavage fluid (BALF) and nasopharyngeal lavage fluid (NLF) samples from RSV-infected infants (26, 27), and neutrophils recovered from these sites display activation markers such as increased CD11b and CD64, and reduced CD62L (28-32). Elevated neutrophil counts in BALF are also associated with severe RSV bronchiolitis in infants (7). In this study, we compared peripheral blood neutrophils from RSV-infected infants with control infants and observed that RSV-infected infants had elevated levels of MPO and NE, suggesting systemic neutrophil activation. Interestingly, these infants exhibited a lower overall neutrophil count in circulation, likely reflecting increased recruitment to the lungs—a well-documented feature of RSV bronchiolitis.

To validate clinical findings, we developed an in vitro co-culture model using differentiated paediatric airway epithelial cells (AECs) and endothelial cells (ECs) to simulate neutrophil extravasation during RSV infection (18). ECs were included to better replicate neutrophil migration across the endothelium in response to inflammation. Their presence did not affect RSV infection of AECs, as viral titres were comparable to models without ECs. RSV infection induced IL-6, IL-8, and IP-10 production above mock levels in both models, which is consistent with previous *in vitro* studies (10, 33). This is also in line with patient data, with elevated IL-6 and IL-8 levels in nasopharyngeal aspirates (NPA) being shown to correlate with RSV disease severity in children (34, 35). Similarly, high levels of CXC chemokines, including IP-10, in BALF from RSV-infected infants further underscore their role in driving pulmonary inflammation (36). Interestingly, the level of these RSV-induced cytokines was significantly lower in the EC compared to the non-EC model, suggesting that ECs may dampen early inflammatory responses via negative feedback. Interestingly, this contrasts with influenza A virus, where ECs have been shown to enhance cytokine production in response to infected epithelial cells (37).

We then found that neutrophil trans-epithelial migration was significantly increased following RSV infection, likely driven by elevated IL-8 and IP-10. Without endothelial cells (ECs), most neutrophils remained attached to RSV-infected airway epithelial cells (AECs), whereas the EC model promoted greater numbers of fully migrated, detached

neutrophils. This supports previous findings (10, 15), and suggests that ECs influence neutrophil behaviour, with detached, migrated neutrophils potentially playing a key role in RSV pathogenesis. Although differences between RSV and mock conditions were not statistically significant, quartile analysis across all markers indicated that migration itself may drive neutrophil activation. Migrated neutrophils displayed a distinct activated phenotype—elevated CD11b, CD64, MPO, and NE, and reduced CD62L—mirroring profiles seen in BALF and peripheral blood neutrophils from RSV-infected infants (28-32, 38). This activation appeared to result from direct contact with RSV-infected AECs rather than soluble factors alone. Notably, basolateral neutrophils that were prevented from migrating did not exhibit these changes, suggesting that trans-epithelial migration is essential for full activation. These findings raise the possibility that basolateral neutrophils may undergo reverse migration, and that traversal across ECs and infected AECs primes them for degranulation—potentially contributing to systemic inflammation by transporting viral components beyond the lung (10, 39, 40).

To determine whether treatment with an antiviral drug could help modulate this response, we tested two well-characterized RSV inhibitors, RDV and RSV604, which target distinct stages of RSV replication (25, 41). We found that both significantly reduced viral load and GFP fluorescence in infected AECs, consistent with previous studies (25, 42). However, the reduction in IL-6 levels with RDV, observed only after neutrophil migration, suggests that the presence of neutrophils, possibly in conjunction with reduced viral antigen load, may contribute to a regulatory feedback mechanism that reduces inflammation thereby improving disease outcomes.

Interestingly, RSV604 increased the number of viable neutrophils migrating across infected co-cultures. Neutrophils play a crucial role in viral clearance, but excessive recruitment and degranulation can cause tissue damage. However, our data indicate that neutrophils migrating under RSV604 treatment were less activated, with reduced expression of CD11b and MPO and increased levels of CD62L. This suggests that RSV604 may promote the recruitment of less activated, "naive" neutrophils, which could mitigate excessive inflammation. Additionally, the effect of RSV604 on CD62L implies that the drug may modulate neutrophil-endothelial interactions during migration, possibly by altering cytokine signalling or endothelial adhesion molecule expression. Further

research is needed to explore how RSV604 influences these pathways and whether it has the potential to modulate neutrophils *in vivo*.

A limitation of this study is the use of paediatric neutrophils for *in vivo* analysis and adult neutrophils for *in vitro* experiments, due to logistical challenges in obtaining healthy paediatric blood samples. Although direct comparison revealed only minor differences in the resting state between healthy paediatric and adult donors (**Supplementary Figure 6),** subtle age-related differences in neutrophil responsiveness or priming potential may still influence the observed outcomes. Additionally, the *in vitro* model, while physiologically relevant, does not fully recapitulate the complexity of the *in vivo* airway environment, including interactions with other immune cell types and systemic factors.

Conclusion

Our study identifies myeloperoxidase (MPO) as a key marker of neutrophil activation and a potential systemic indicator of disease severity in RSV infection. Using a clinically informed *in vitro* model, we showed that neutrophil activation is primarily driven by direct contact with RSV-infected epithelial cells, resulting in increased expression of CD11b, MPO, and NE, and reduced CD62L—features associated with severe disease. MPO emerged as the most significantly modulated marker, confirmed by both expression and enzymatic activity assays. Although both RDV and RSV604 reduced MPO levels compared to RSV alone, neither restored them to baseline, indicating only partial suppression of degranulation. Notably, RSV604—but not RDV—reduced MPO expression more effectively, suggesting its potential to mitigate neutrophil-mediated tissue damage. Furthermore, high MPO expression in basolateral, reverse-migrated neutrophils points to a possible role in systemic inflammation. These results suggest that neutrophil MPO expression should be considered a relevant biomarker in the evaluation and screening of antiviral therapies for RSV.

Acknowledgements

This study was funded by Animal Free Research UK (AFR19-20274) and was carried out in accordance with the terms and conditions as stated in document number GH2019-TC/v1.1/27.01.2020. We would like to thank the members of the research nursing team at GOSH, including Lauren O'Neill, Holly Bellfield, Shannon McCarty, Kate Plant and Sarah Benkenstein, who helped with patient screening and sample collection. This work was supported by the NIHR Great Ormond Street Hospital Biomedical Research Centre. We are grateful to Cecilia Johannssen for her guidance during initial project development and for review of the manuscript. The views expressed are those of the author(s) and not necessarily those of the NHS, the NIHR or the Department of Health. C.M.S also acknowledges funding support from UKRI/ BBSRC (BB/V006738/1).

Author contributions

M.P. designed the study, conducted experiments, analysed data, and co-wrote the manuscript. S.E. and A.I.J. contributed to study design, conducted experiments and provided access to reagents. S.E. also assisted in reviewing the manuscript. T.B. and P.D.C. contributed to study design and provided access to reagents. C.M.S. and S.R. provided support through ethics and patient recruitment. R.L.S. and C.M.S. conceived the study and oversaw the funding application. J.L.R. and G.P. contributed to data analysis (quartile scoring). C.M.S. contributed to study design and co-wrote the manuscript. M.P., R.E.H., and C.M.S. oversaw data analysis, interpretation, and the manuscript write-up.

Code availability

Custom code for the analysis performed in this study will be made publicly available via GitHub at https://github.com/smithlab-code.

Table 1. PICU Patient Demographics

Patient ID	Ethnicity	Age	Sex	Group	Additional Information (i.e, microbiology)	Other Relevant Medical Notes	Neutrophil Count (cells/ml blood)
1006	White British	15 months	F	RSV	Paediatric acute respiratory distress syndrome (PARDS) on high support		8.50×10^5
					Prior rhino/enterovirus		
					Adenovirus NPA currently negative		
					**started on low dose steroids, favipiravir/ nitazoxanide/ribavirin after sample was taken*		
1081	White British	2 months	F	RSV	Worsening type 2 respiratory failure, diagnosed as RSV bronchiolitis	Premature birth at 27 weeks	9.50×10^5
1082	White British	3 months	F	RSV	Bronchiolitis - RSV B positive	Premature birth at 31+3 weeks	3.50×10^5
					PARDS	Large neck capillary haemangioma	
						Large atrial septal defect	
1083	Other Mixed Background	29 months	M	RSV	Bronchiolitis - RSV A/B positive	Ex 34+0/40	2.18×10^6
						Chromosomal abnormality	
					PARDS	Pierre Robin sequence, cleft palate, previous Grade 3 airway	
						Chronic liver disease, obstructive sleep apnea, nocturnal BiPAP (Resmed) 18/10, off oxygen since April 2023	
					Recent history of flu B	Nissen fundoplication + gastrostomy	
						Non-obstructive RV rhabdomyoma (last echo Oct 2023), no compromise	
						NEC post-natally - ileostomy and colostomy reversed (2021)	
1084	Other White Background	6 weeks	M	RSV	RSV A/B positive	Born at term, no neonatal concerns	6.30×10^5
					Rhino/enterovirus positive		
1085	White British	5 months	F	DC	Recurrent aspiration related lung infections, currently none	VACTERL with oesophageal atresia, sample D2 post repair	1.80×10^6
						Chronic kidney disease, on long term renal replacement	
1086	White British	7 months	M	DC	Vein of Galen malformation, D1 post 2nd embolization (not ventilated)		1.60×10^6
1087	Other Mixed Background	1 week	F	DC	Polycystic kidney disease, lung hypoplasia		3.00×10^6
1088	White British	4 weeks	F	DC	Atrioventricular septal defect, coarctation of aorta (D1 post coarctation repair and pulmonary artery band)		2.80×10^6
1089	Asian British - Indian	2 months	F	DC	Lymphatic malformation	Post sclerotherapy, not ventilated	2.40×10^6

References

1. Shi T, McAllister DA, O'Brien KL, Simoes EAF, Madhi SA, Gessner BD, et al. Global, regional, and national disease burden estimates of acute lower respiratory infections due to respiratory syncytial virus in young children in 2015: a systematic review and modelling study. Lancet. 2017;390(10098):946-58.
2. Frankel LR, Wilson CW, Demers RR, Parker JR, Lewiston NJ, Stevenson DK, et al. A technique for the administration of ribavirin to mechanically ventilated infants with severe respiratory syncytial virus infection. Crit Care Med. 1987;15(11):1051-4.
3. American Academy of Pediatrics Committee on Infectious D, American Academy of Pediatrics Bronchiolitis Guidelines C. Updated guidance for palivizumab prophylaxis among infants and young children at increased risk of hospitalization for respiratory syncytial virus infection. Pediatrics. 2014;134(2):415-20.
4. Subramanian KN, Weisman LE, Rhodes T, Ariagno R, Sanchez PJ, Steichen J, et al. Safety, tolerance and pharmacokinetics of a humanized monoclonal antibody to respiratory syncytial virus in premature infants and infants with bronchopulmonary dysplasia. MEDI-493 Study Group. Pediatr Infect Dis J. 1998;17(2):110-5.
5. Griffin MP, Yuan Y, Takas T, Domachowske JB, Madhi SA, Manzoni P, et al. Single-Dose Nirsevimab for Prevention of RSV in Preterm Infants. N Engl J Med. 2020;383(5):415-25.
6. Hammitt LL, Dagan R, Yuan Y, Baca Cots M, Bosheva M, Madhi SA, et al. Nirsevimab for Prevention of RSV in Healthy Late-Preterm and Term Infants. N Engl J Med. 2022;386(9):837-46.
7. McNamara PS, Ritson P, Selby A, Hart CA, Smyth RL. Bronchoalveolar lavage cellularity in infants with severe respiratory syncytial virus bronchiolitis. Arch Dis Child. 2003;88(10):922-6.
8. Wang SZ, Xu H, Wraith A, Bowden JJ, Alpers JH, Forsyth KD. Neutrophils induce damage to respiratory epithelial cells infected with respiratory syncytial virus. Eur Respir J. 1998;12(3):612-8.
9. Kirsebom FCM, Kausar F, Nuriev R, Makris S, Johansson C. Neutrophil recruitment and activation are differentially dependent on MyD88/TRIF and MAVS signaling during RSV infection. Mucosal Immunol. 2019;12(5):1244-55.
10. Robinson E, Herbert JA, Palor M, Ren L, Larken I, Patel A, et al. Trans-epithelial migration is essential for neutrophil activation during RSV infection. J Leukoc Biol. 2023;113(4):354-64.
11. Robinson E, Sawhney S, Cortina-Borja M, David AL, Smith CM, Smyth RL. Neutrophil responses to RSV infection show differences between infant and adult neutrophils. Thorax. 2024;79(6):545-52.
12. Halfhide CP, Flanagan BF, Brearey SP, Hunt JA, Fonceca AM, McNamara PS, et al. Respiratory syncytial virus binds and undergoes transcription in neutrophils from the blood and airways of infants with severe bronchiolitis. J Infect Dis. 2011;204(3):451-8.
13. Zemans RL, Colgan SP, Downey GP. Transepithelial migration of neutrophils: mechanisms and implications for acute lung injury. Am J Respir Cell Mol Biol. 2009;40(5):519-35.

14. Taylor G. Animal models of respiratory syncytial virus infection. Vaccine. 2017;35(3):469-80.
15. Herbert JA, Deng Y, Hardelid P, Robinson E, Ren L, Moulding D, et al. beta(2)-integrin LFA1 mediates airway damage following neutrophil transepithelial migration during respiratory syncytial virus infection. Eur Respir J. 2020;56(2).
16. Butler CR, Hynds RE, Gowers KH, Lee Ddo H, Brown JM, Crowley C, et al. Rapid Expansion of Human Epithelial Stem Cells Suitable for Airway Tissue Engineering. Am J Respir Crit Care Med. 2016;194(2):156-68.
17. Hynds RE, Butler CR, Janes SM, Giangreco A. Expansion of Human Airway Basal Stem Cells and Their Differentiation as 3D Tracheospheres. Methods Mol Biol. 2019;1576:43-53.
18. Palor M, Haughey, E. K., Herbert, J., O'Callaghan, C., Smyth, R. L., De Coppi, P., Hynds, R. E., & Smith, C. M. Ciliated epithelial cell differentiation at air-liquid interface and RSV infection using animal-free media and substrates. ERJ Open Research. 2025;Accepted for publication.
19. Palikuqi B, Nguyen DT, Li G, Schreiner R, Pellegata AF, Liu Y, et al. Adaptable haemodynamic endothelial cells for organogenesis and tumorigenesis. Nature. 2020;585(7825):426-32.
20. Fix J, Galloux M, Blondot ML, Eleouet JF. The insertion of fluorescent proteins in a variable region of respiratory syncytial virus L polymerase results in fluorescent and functional enzymes but with reduced activities. Open Virol J. 2011;5:103-8.
21. Castagne N, Barbier A, Bernard J, Rezaei H, Huet JC, Henry C, et al. Biochemical characterization of the respiratory syncytial virus P-P and P-N protein complexes and localization of the P protein oligomerization domain. J Gen Virol. 2004;85(Pt 6):1643-53.
22. Nakazawa M. fmsb: Functions for Medical Statistics Book with some Demographic Data. R package version 0.7.6. 2024.
23. Haeberle HA, Takizawa R, Casola A, Brasier AR, Dieterich HJ, Van Rooijen N, et al. Respiratory syncytial virus-induced activation of nuclear factor-kappaB in the lung involves alveolar macrophages and toll-like receptor 4-dependent pathways. J Infect Dis. 2002;186(9):1199-206.
24. Ouyang Y, Liao H, Hu Y, Luo K, Hu S, Zhu H. Innate Immune Evasion by Human Respiratory Syncytial Virus. Front Microbiol. 2022;13:865592.
25. Chapman J, Abbott E, Alber DG, Baxter RC, Bithell SK, Henderson EA, et al. RSV604, a novel inhibitor of respiratory syncytial virus replication. Antimicrob Agents Chemother. 2007;51(9):3346-53.
26. Emboriadou M, Hatzistilianou M, Magnisali C, Sakelaropoulou A, Exintari M, Conti P, et al. Human neutrophil elastase in RSV bronchiolitis. Ann Clin Lab Sci. 2007;37(1):79-84.
27. Sigurs N, Bjarnason R, Sigurbergsson F. Eosinophil cationic protein in nasal secretion and in serum and myeloperoxidase in serum in respiratory syncytial virus bronchiolitis: relation to asthma and atopy. Acta Paediatr. 1994;83(11):1151-5.
28. Cassatella MA, Ostberg NK, Tamassia N, Soehnlein O. Biological Roles of Neutrophil-Derived Granule Proteins and Cytokines. Trends Immunol. 2019;40(7):648-64.
29. Cowland JB, Borregaard N. Granulopoiesis and granules of human neutrophils. Immunol Rev. 2016;273(1):11-28.

30. Hoffmann JJ. Neutrophil CD64: a diagnostic marker for infection and sepsis. Clin Chem Lab Med. 2009;47(8):903-16.
31. Simon SI, Burns AR, Taylor AD, Gopalan PK, Lynam EB, Sklar LA, et al. L-selectin (CD62L) cross-linking signals neutrophil adhesive functions via the Mac-1 (CD11b/CD18) beta 2-integrin. J Immunol. 1995;155(3):1502-14.
32. Weirich E, Rabin RL, Maldonado Y, Benitz W, Modler S, Herzenberg LA, et al. Neutrophil CD11b expression as a diagnostic marker for early-onset neonatal infection. J Pediatr. 1998;132(3 Pt 1):445-51.
33. Villenave R, O'Donoghue D, Thavagnanam S, Touzelet O, Skibinski G, Heaney LG, et al. Differential cytopathogenesis of respiratory syncytial virus prototypic and clinical isolates in primary pediatric bronchial epithelial cells. Virol J. 2011;8:43.
34. Tabarani CM, Bonville CA, Suryadevara M, Branigan P, Wang D, Huang D, et al. Novel inflammatory markers, clinical risk factors and virus type associated with severe respiratory syncytial virus infection. Pediatr Infect Dis J. 2013;32(12):e437-42.
35. Diaz PV, Gaggero AA, Pinto RA, Mamani R, Uasapud PA, Bono MR. [Levels of inflammatory cytokines and plasma cortisol in respiratory syncytial virus bronchiolitis]. Rev Med Chil. 2013;141(5):574-81.
36. McNamara PS, Flanagan BF, Hart CA, Smyth RL. Production of chemokines in the lungs of infants with severe respiratory syncytial virus bronchiolitis. J Infect Dis. 2005;191(8):1225-32.
37. Bauer L, Rijsbergen LC, Leijten L, Benavides FF, Noack D, Lamers MM, et al. The pro-inflammatory response to influenza A virus infection is fueled by endothelial cells. Life Sci Alliance. 2023;6(7).
38. Halfhide CP, Brearey SP, Flanagan BF, Hunt JA, Howarth D, Cummerson J, et al. Neutrophil TLR4 expression is reduced in the airways of infants with severe bronchiolitis. Thorax. 2009;64(9):798-805.
39. Nourshargh S, Renshaw SA, Imhof BA. Reverse Migration of Neutrophils: Where, When, How, and Why? Trends Immunol. 2016;37(5):273-86.
40. Buckley CD, Ross EA, McGettrick HM, Osborne CE, Haworth O, Schmutz C, et al. Identification of a phenotypically and functionally distinct population of long-lived neutrophils in a model of reverse endothelial migration. J Leukoc Biol. 2006;79(2):303-11.
41. Frediansyah A, Nainu F, Dhama K, Mudatsir M, Harapan H. Remdesivir and its antiviral activity against COVID-19: A systematic review. Clin Epidemiol Glob Health. 2021;9:123-7.
42. Warren TK, Jordan R, Lo MK, Ray AS, Mackman RL, Soloveva V, et al. Therapeutic efficacy of the small molecule GS-5734 against Ebola virus in rhesus monkeys. Nature. 2016;531(7594):381-5.

Figure 1

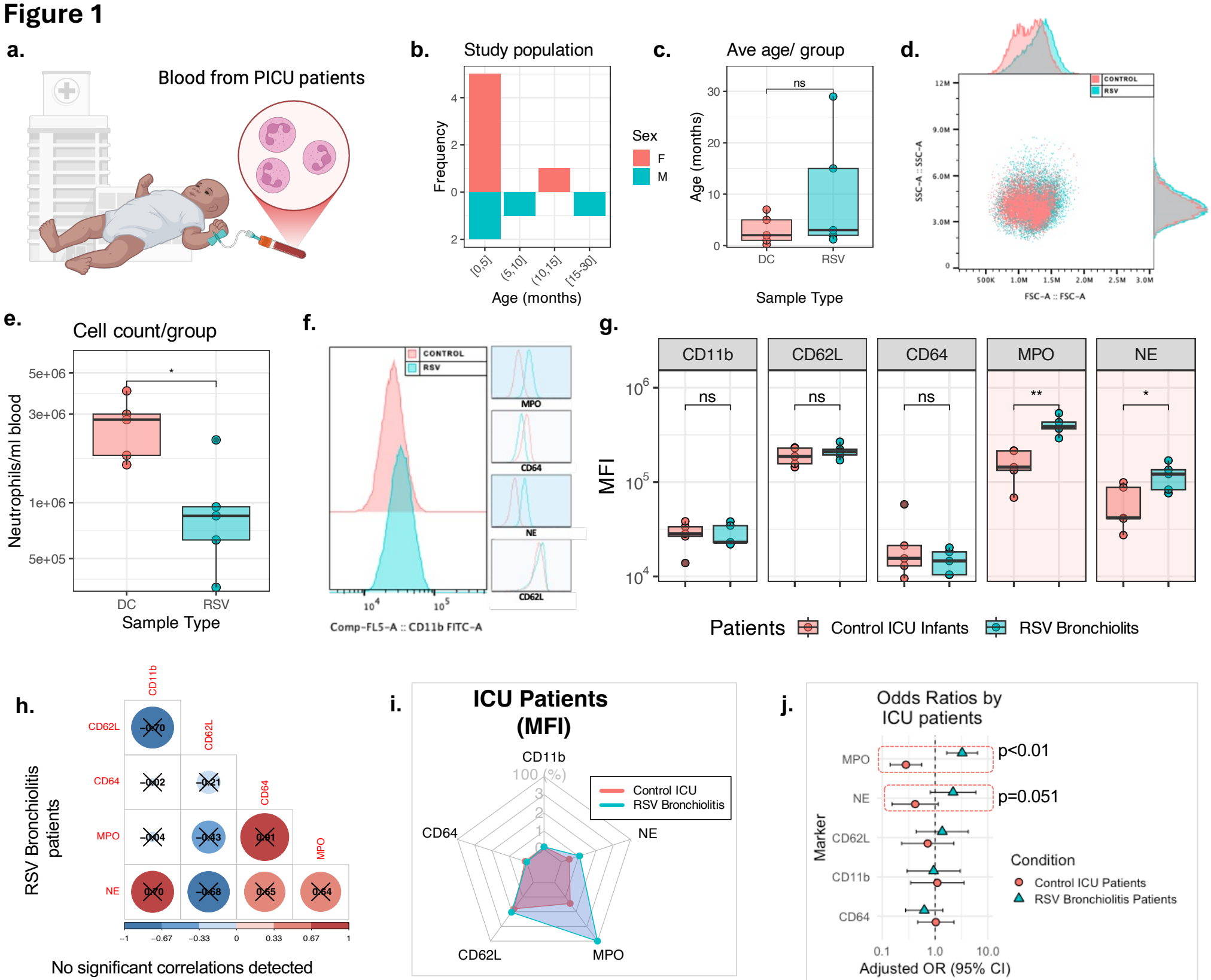
a.
Blood from PICU patients
b.
Study population
Frequency
Sex
F
M
[0,5]
(5,10]
(10,15]
[15-30]
Age (months)
c.
Ave age/ group
ns
Age (months)
DC
RSV
Sample Type
d.
CONTROL
RSV
SSC-A :: SSC-A
FSC-A :: FSC-A
e.
Cell count/group
Neutrophils/ml blood
DC
RSV
Sample Type
f.
CONTROL
RSV
MPO
CD64
NE
CD62L
Comp-FL5-A :: CD11b FITC-A
g.
CD11b
CD62L
CD64
MPO
NE
MFI
ns
**
*
Patients
Control ICU Infants
RSV Bronchiolits
h.
RSV Bronchiolitis patients
CD62L
CD64
MPO
NE
No significant correlations detected
i.
ICU Patients (MFI)
CD11b
CD64
NE
CD62L
MPO
Control ICU
RSV Bronchiolitis
j.
Odds Ratios by ICU patients
MPO
NE
CD62L
CD11b
CD64
p<0.01
p=0.051
Marker
Condition
Control ICU Patients
RSV Bronchiolitis Patients
Adjusted OR (95% CI)

Figure 2

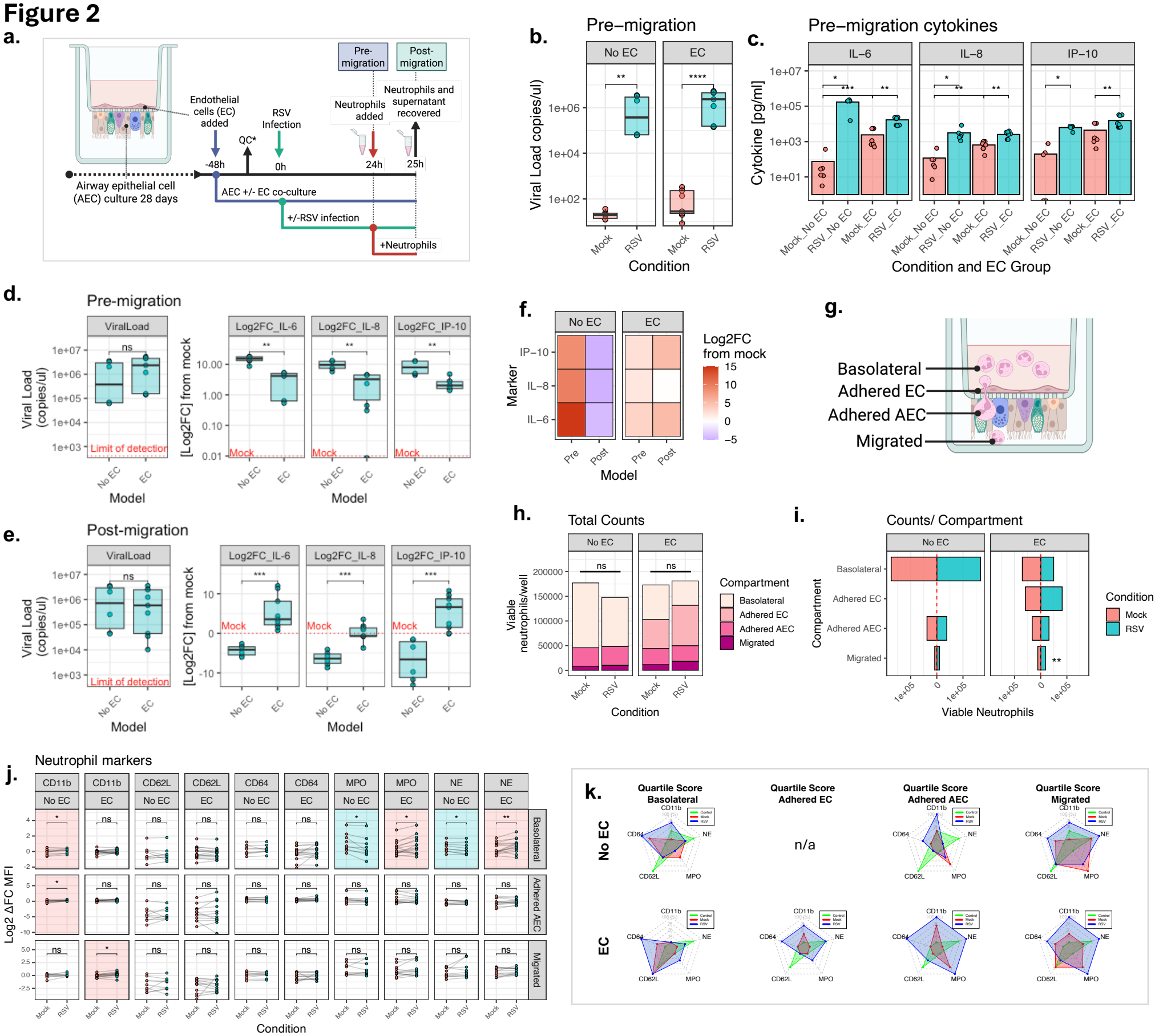
a.
Pre-migration
Post-migration
Endothelial cells (EC) added
RSV Infection
Neutrophils added
Neutrophils and supernatant recovered
QC*
-48h
0h
24h
25h
Airway epithelial cell (AEC) culture 28 days
AEC +/- EC co-culture
+/-RSV infection
+Neutrophils
b.
Pre–migration
No EC
EC
Viral Load copies/ul)
Mock
RSV
Condition
c.
Pre–migration cytokines
IL–6
IL–8
IP–10
Cytokine [pg/ml]
Mock_No EC
RSV_No EC
Mock_EC
RSV_EC
Condition and EC Group
d.
Pre-migration
ViralLoad
Log2FC_IL-6
Log2FC_IL-8
Log2FC_IP-10
Viral Load (copies/ul)
[Log2FC] from mock
Limit of detection
Mock
No EC
EC
Model
e.
Post-migration
f.
Marker
Log2FC from mock
Pre
Post
g.
Basolateral
Adhered EC
Adhered AEC
Migrated
h.
Total Counts
Viable neutrophils/well
Compartment
i.
Counts/ Compartment
Condition
Viable Neutrophils
j.
Neutrophil markers
CD11b
CD62L
CD64
MPO
NE
Log2 ΔFC MFI
k.
Quartile Score Basolateral
Quartile Score Adhered EC
Quartile Score Adhered AEC
Quartile Score Migrated
n/a

Figure 3

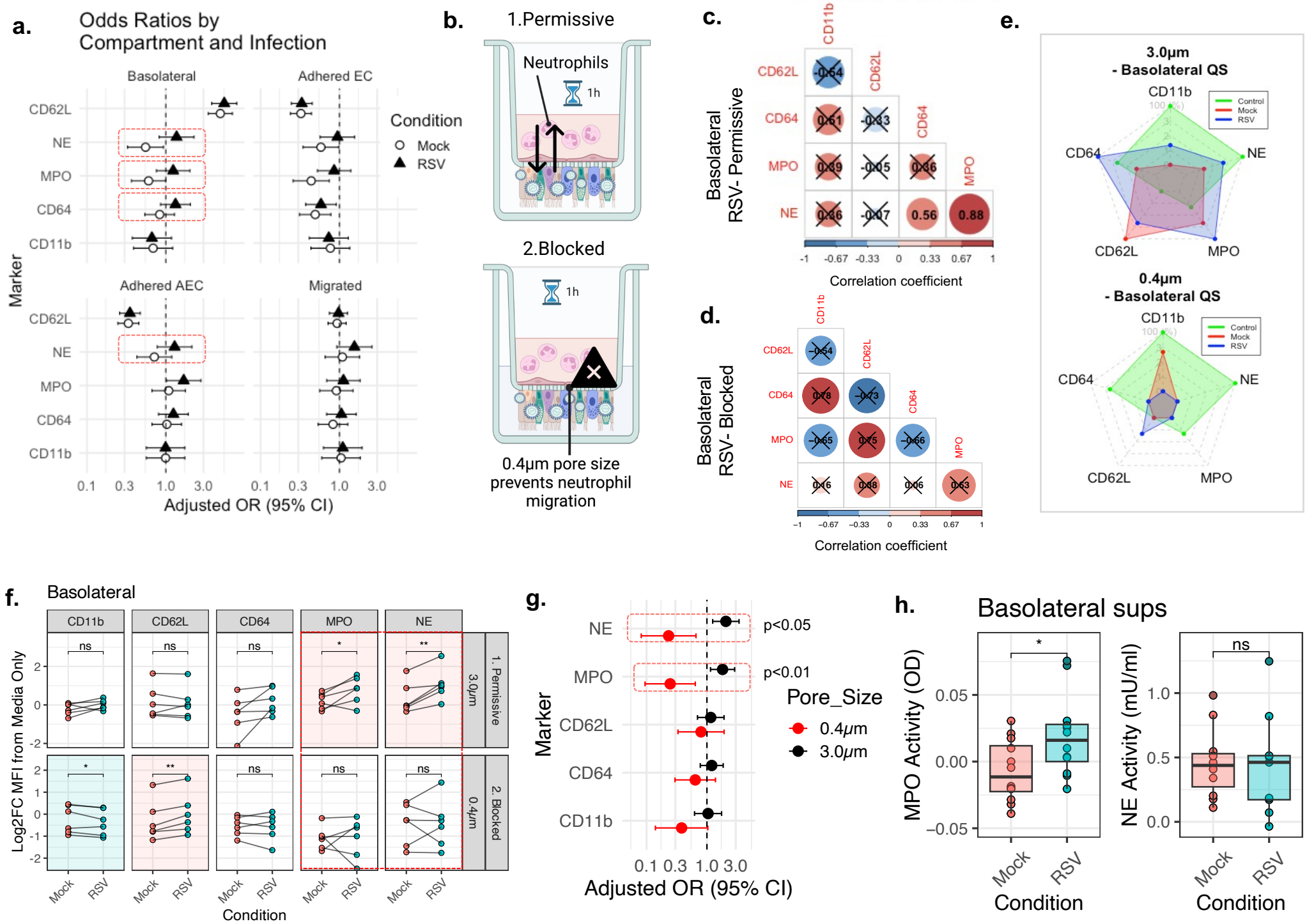
a.
Odds Ratios by Compartment and Infection
Basolateral
Adhered EC
Adhered AEC
Migrated
CD62L
NE
MPO
CD64
CD11b
Marker
Condition
Mock
RSV
0.1 0.3 1.0 3.0
Adjusted OR (95% CI)
b.
1.Permissive
Neutrophils
1h
2.Blocked
1h
0.4µm pore size prevents neutrophil migration
c.
Basolateral RSV- Permissive
CD11b
CD62L
CD64
MPO
NE
-0.54
0.61
-0.33
0.39
-0.05
0.36
0.36
-0.07
0.56
0.88
-1 -0.67 -0.33 0 0.33 0.67 1
Correlation coefficient
d.
Basolateral RSV- Blocked
CD11b
CD62L
CD64
MPO
NE
-0.54
0.78
-0.73
-0.65
0.75
-0.66
0.16
0.68
0.06
0.63
−1 −0.67 −0.33 0 0.33 0.67 1
Correlation coefficient
e.
3.0µm - Basolateral QS
CD11b
CD64
NE
CD62L
MPO
Control
Mock
RSV
0.4µm - Basolateral QS
CD11b
CD64
NE
CD62L
MPO
Control
Mock
RSV
f.
Basolateral
CD11b
CD62L
CD64
MPO
NE
ns
*
**
1. Permissive 3.0µm
2. Blocked 0.4µm
Log2FC MFI from Media Only
Mock
RSV
Condition
g.
NE
MPO
CD62L
CD64
CD11b
p<0.05
p<0.01
Pore_Size
0.4µm
3.0µm
Marker
0.1 0.3 1.0 3.0
Adjusted OR (95% CI)
h.
Basolateral sups
MPO Activity (OD)
NE Activity (mU/ml)
*
ns
Mock
RSV
Condition

Figure 4

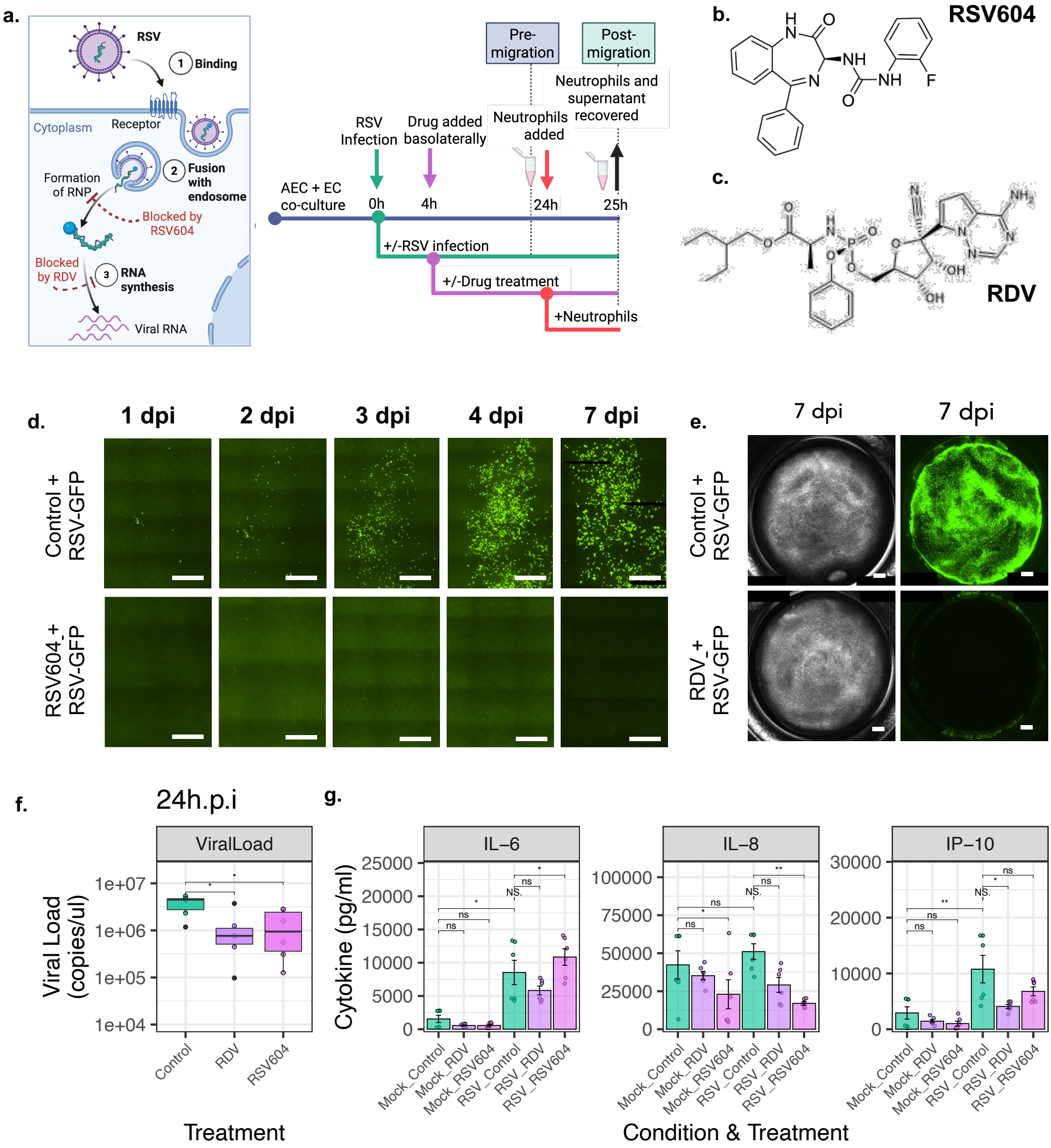
a.
RSV
1 Binding
Cytoplasm
Receptor
Formation of RNP
2 Fusion with endosome
Blocked by RSV604
Blocked by RDV
3 RNA synthesis
Viral RNA
Pre-migration
Post-migration
Neutrophils and supernatant recovered
Neutrophils added
RSV Infection
Drug added basolaterally
AEC + EC co-culture
0h
4h
24h
25h
+/-RSV infection
+/-Drug treatment
+Neutrophils
b.
RSV604
c.
RDV
d.
1 dpi
2 dpi
3 dpi
4 dpi
7 dpi
Control + RSV-GFP
RSV604 + RSV-GFP
e.
7 dpi
7 dpi
Control + RSV-GFP
RDV + RSV-GFP
f.
24h.p.i
ViralLoad
Viral Load (copies/ul)
1e+07
1e+06
1e+05
1e+04
Control
RDV
RSV604
Treatment
g.
IL−6
IL−8
IP−10
Cytokine (pg/ml)
25000
20000
15000
10000
5000
0
100000
75000
50000
25000
30000
20000
10000
ns
NS.
Mock_Control
Mock_RDV
Mock_RSV604
RSV_Control
RSV_RDV
RSV_RSV604
Condition & Treatment

Figure 5

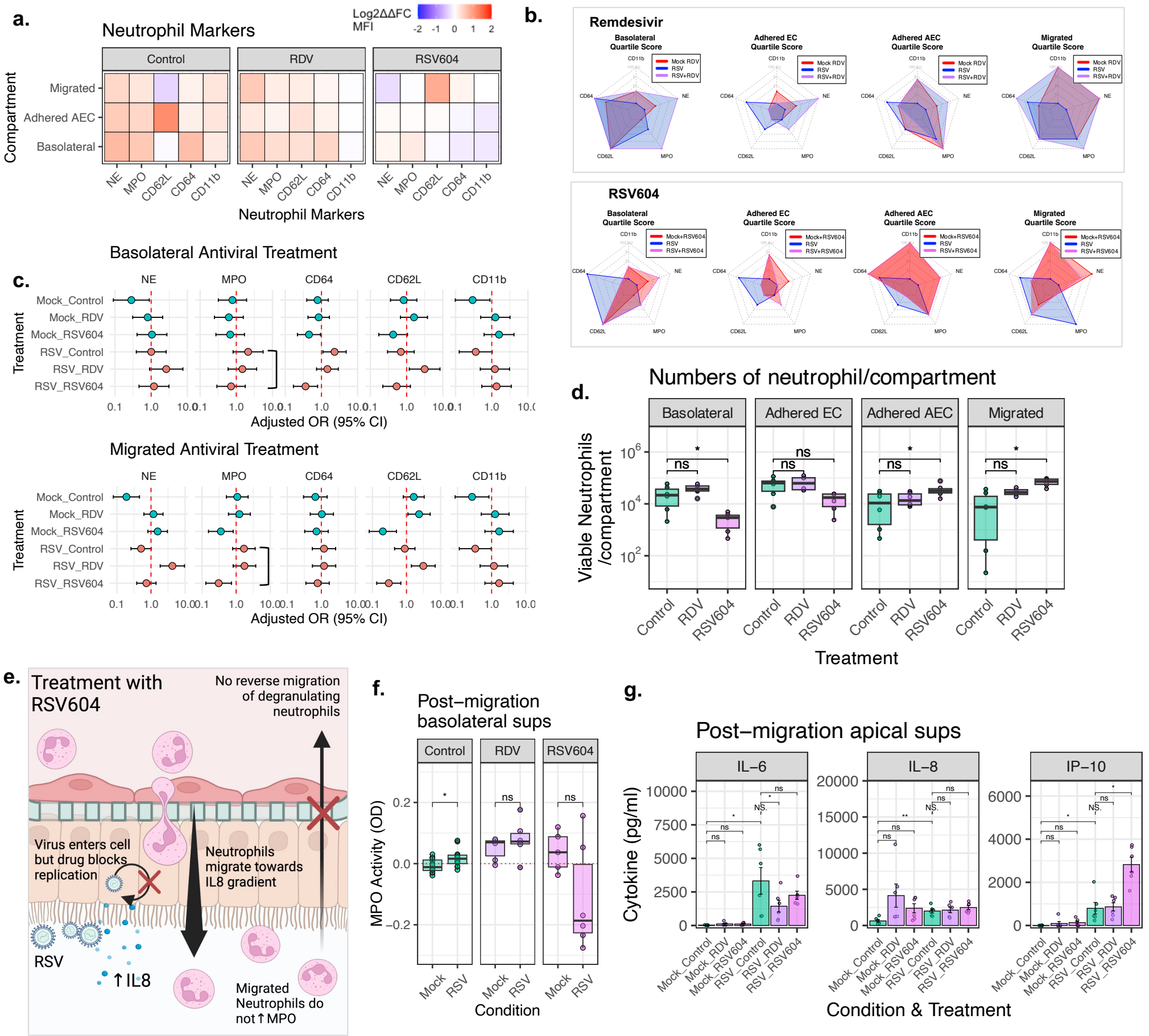
a.
Neutrophil Markers
Log2ΔΔFC MFI
-2 -1 0 1 2
Control
RDV
RSV604
Compartment
Migrated
Adhered AEC
Basolateral
NE
MPO
CD62L
CD64
CD11b
Neutrophil Markers
b.
Remdesivir
Basolateral Quartile Score
Adhered EC Quartile Score
Adhered AEC Quartile Score
Migrated Quartile Score
Mock RDV
RSV
RSV+RDV
RSV604
Mock+RSV604
RSV+RSV604
c.
Basolateral Antiviral Treatment
Treatment
Mock_Control
Mock_RDV
Mock_RSV604
RSV_Control
RSV_RDV
RSV_RSV604
Adjusted OR (95% CI)
Migrated Antiviral Treatment
d.
Numbers of neutrophil/compartment
Basolateral
Adhered EC
Adhered AEC
Migrated
Viable Neutrophils /compartment
ns
*
Treatment
e.
Treatment with RSV604
No reverse migration of degranulating neutrophils
Virus enters cell but drug blocks replication
Neutrophils migrate towards IL8 gradient
RSV
↑IL8
Migrated Neutrophils do not ↑MPO
f.
Post–migration basolateral sups
MPO Activity (OD)
Condition
Mock
RSV
g.
Post–migration apical sups
IL–6
IL–8
IP–10
Cytokine (pg/ml)
Condition & Treatment